# A Reconfigurable Interconnect Technology based on Spoof Plasmon

#### Soumitra Roy Joy

Electrical Engineering and Computer Science
University of Michigan
Ann Arbor, MI, USA
srjoy@umich.edu

#### Md Zunaid Baten

Electrical and Electronic Engineering
Bangladesh University of Engineering & Technology
Dhaka, Bangladesh
mdzunaid@ieee.org

#### Pinaki Mazumder

Electrical Engineering and Computer Science
University of Michigan
Ann Arbor, MI, USA
pinakimazum@gmail.com

#### Md Faizul Bari

Electrical and Electronic Engineering
Bangladesh University of Engineering & Technology
Dhaka, Bangladesh
faizul.eee.buet@gmail.com

Feng Lan

Electrical Engineering and Computer Science
University of Michigan
Ann Arbor, MI, USA
fenglan@umich.edu

Abstract—The bottleneck of inter-chip communication speed, for instance that between logic and memory units is a long standing issue in acquiring ultra-fast computing. While research from two extreme end of technologies: electrical, and optical interconnect have their own pitfall in constructing an energyeconomic route of communication with high bandwidth density, a radically different technology named as spoof plasmon based communication may bring new insight towards addressing the issue. This technology smoothly interweaves the advantages of electrical interconnect and that of optical ones. In the present work, we have given a proof-of-concept demonstration of the signal transfer capacity of spoof plasmon parallel data-bus. We demonstrated that spoof plasmon channel can accommodate two different kinds of mode: electro-SSPP mode and opto-SSPP mode. Depending on the data-traffic, SSPP channel can be dynamically reconfigured for supporting either of the two modes for information transfer in order to minimize energy consumption. In addition, we also endeavored to answer to the question that whether the metasurface based information transfer system can be reliable in case of patterning irregularity induced by fabrication process variations.

*Index Terms*—spoof plasmon, interconnect, reconfigurability, cross-talk, process variation

#### I. INTRODUCTION

The inter-chip communication technology until now has been mainly explored in the low ( $\leq$  200 GHz) frequency regime of electronics [1], [2] and the high-frequency regime of optics (200-800 THz) [3], [4], leaving the intermediate terahertz frequency region (300 GHz to 10 THz) underexploited and under-utilized [10]. In the present work, the authors aim at assessing the potential of a novel technique of communication technology for the untapped THz regime. The technology involves spoof surface plasmon polariton:

a special form of electromagnetic mode over metamaterial interconnect for information transfer at terahertz frequency.

The technique is based on the fact that a metal wire with special design of sub-wavelength patterns can support propagation of confined electromagnetic mode, which can get rid of the main bottlenecks of the performance of standard metallic interconnects arising from RC-time delay, cross-talk, parasitic capacitance, and inductance effects. The authors have earlier demonstrated the capability of THz surface wave interconnect in multiple recent publications [5], [8]. At THz frequency, a signal can transfer information to a significant distance (up to tens of centimeters) with very low attenuation and cross-talk between wires [5], [11]. This property of SSPP can be leveraged to transfer data at 100s of Gigabit per second (Gbps) speed among different chips on a multi-chip module (MCM) carrier or system-on-chip (SoC) packaging.

It has been shown by Cho et al. [6] that, at tens of Gbps speed, there lies a critical zone at centimeter range of interconnect length where either optical or electrical solution for inter-chip communications fails to provide the optimal performance. The interconnect technologists call the bottleneck as the 'last centimeter' problem [9]. The 'last centimeter' problem exacerbates further critical due to statistical variations of data traffic over a time period, which poses a dilemma in choosing the optimal mode of data transfer.

In order to circumvent the unresolved problem, we envision implementing a hybrid mode of data transfer that can be dynamically reconfigured to support two different types of modes on the same physical channel. In this technology, the interconnect propagates information in the form of spoof

surface plasmon polariton, a quasiparticle that derives its name due to its behavioral similarity to conventional surface plasmon polariton found in the optical and near-infrared regimes. The authors have predicted that THz surface wave (SSPP) interconnects comprising patterned metallic wire can simultaneously accommodate low-power baseband mode analogous to electronic signal and high-bandwidth mode analogous to optical signal [5]. Therefore, one can design the system architecture so that, depending on the traffic at a given time, the physical channel will dynamically select the electronic or optical mode to match the energy-efficient mechanism of information transfer at the present data-rate. In this work, the authors have validated their earlier prediction of reconfigurability between two different modes in SSPP channel by experiments. The study also takes into account the effect of inadvertent irregularity in the patterning in SSPP interconnect: a practical concern arisen from fabrication process variation. Such an innovative approach is expected to provide a new roadmap for short-range interconnects with high data rate and low energy budget.

### II. WHY DO WE NEED RECONFIGURABLE INTERCONNECT?: A COMPARATIVE ANALYSIS

In order to appreciate the need of a reconfigurable interconnect, we have to analyze first the limitation of parallel databus electrical interconnect of protecting signal integrity from cross-talk, and compare it with that of SSPP based parallel data-bus.

#### A. Cross-talk in electrical interconnects

For inter-chip communication implemented through purely electrical interconnects, we can analyze its bandwidth density by modeling the interconnect network as a distributed RLCG circuit, where R, L, C, G are defined as resistance, selfinductance, capacitance, and conductance of the dielectric, per unit length, respectively. Each interconnect is coupled to its nearest neighbor through mutual inductance M and mutual capacitance D, also defined per unit length.

It can be shown that the -3 dB cross-talk length  $l_{x,el}$  in such a system is [5],

$$l_{x,el} = \frac{\pi}{2} \frac{1}{\sqrt{\omega RC}} \frac{C}{D} \tag{1}$$

The above expression can also be written in terms of bandwidth  $(2\pi \times BW_{el} = \omega_c = \frac{1}{RCL^2})$  of the electrical channel of length L, as follows

$$l_{x,el} = \frac{\pi}{2} \sqrt{\frac{\omega_c}{\omega}} \frac{C}{D} L \tag{2}$$

The expression of  $l_{x,el}$  shows that signal contamination by cross-talk in an electrical interconnects network aggravates as the ratio  $\frac{D}{C}$  increases. The ratio of mutual capacitance to selfcapacitance increases if the spacing between the neighbor interconnects reduces. In addition, there is an inverse squareroot relation between critical cross-talk length  $l_{x,el}$  and the operating frequency  $\omega$ . This relation in particular shows why electrical interconnects at higher frequencies become

more vulnareble to cross-talk. Figure 2 shows the maximum allowable length for an electrical interconnect in order to avoid cross-talk. The diagram is drawn for a group of parallel data-bus characterized by the ratio of mutual- and selfcapacitance  $(\frac{D}{C})$ . In electrical channels, beyond a critical frequency, shown in red circle in Fig. 2, the cross-talk can become so severe that the undesired signal strength in the victim channel exceeds the signal strength in the intended channel. If we arrange the parallel data-bus denser in an attempt to increase bandwidth density, this critical frequency, will shift further left as the  $\frac{D}{C}$  ratio increases.

#### B. Cross-talk in Spoof Plasmon Interconnects

SSPP interconnects can be appreciably coupled only if they are poised face-to-face (i.e., there is essentially no coupling between back-to-back SSPP interconnect pair). It can be shown that, the coupling factor  $K_{sp}$  between two identical SSPP channels poised face-to-face obeys the following rela-

$$K_{sp} = 2tn_{eff}^2 \frac{\beta^2 \kappa^2 + (\beta^2 - k^2)^2}{\beta \kappa} e^{-2\kappa t}$$
 (3)

where  $\kappa$  is the evanescent decay rate of the field on the SSPP surface. It can be shown that, the cross-talk free length  $l_{x,sp}$ 

is related to the coupling constant as,  $l_{x,sp}=\frac{\pi}{4}\frac{1}{|K_{sp}|}.$  In the limiting case of  $\frac{2\omega}{h}c \to \pi$ , critical cross-talk length in SSPP interconnects become

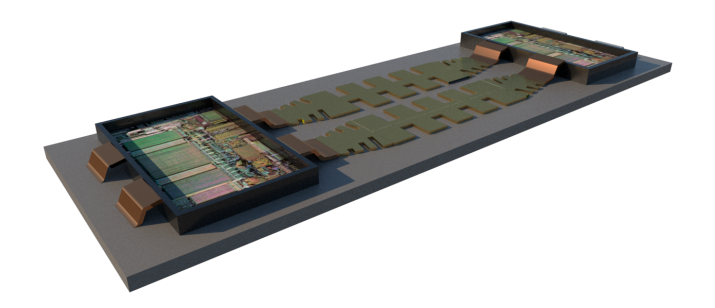
$$\lim_{2\omega h \to \pi c} l_{x,sp} \sim \exp\left[\frac{\pi}{h} \frac{a}{d} \frac{2tc}{\pi c - 2\omega h}\right] \tag{4}$$

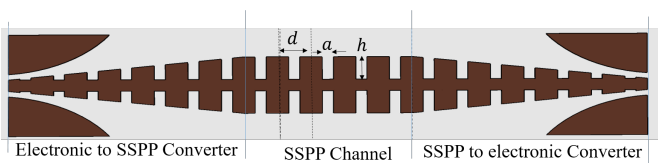
The above expression of critical cross-talk length in SSPP interconnects system reveals that,  $l_{x,sp}$  diverges at a frequency  $\omega = \frac{\pi c}{2h}$ . Thus we can achieve cross-talk suppression at a chosen high frequency by tailoring the geometry of SSPP structure, particularly the length h of the groove.

Figure 3 illustrates the maximum length of interconnect that can remain necessarily unaffected by cross-talk at different frequencies in an arrangement of parallel SSPP channels. A typical geometry of SSPP interconnects system is chosen with groove length of  $h=250~\mu m$  and period of  $d=375~\mu m$ . The spacing between neighboring interconnect is taken as  $2h \mu m$ . It shows that, SSPP interconnect demonstrates quite opposite trend of cross-talk suppression compared to electrical interconnect: cross-talk in SSPP decreases with increasing frequencies, until we reach the band-edge frequency of SSPP channel. Thus SSPP interconnect can be a superior choice over conventional electrical interconnect in circumstances where signal integrity is mainly limited by cross-interference among the nearby channels.

#### C. How critical is the cross-talk?

To illustrate how severely the cross-talk alone can affect the signal integrity in a dense array of parallel electrical channels, we simulated two parallel electrical wires with ideal conductivity, supported by a ground plane at the bottom of the substrate, with the following geometry: length of wire





(b) Geometric features of SSPP channel, including the converter

(a) Illustration of high speed chip-to-chip communication by spoof plasmon interconnect

Fig. 1: Spoof plasmon channel for data transfer among chips

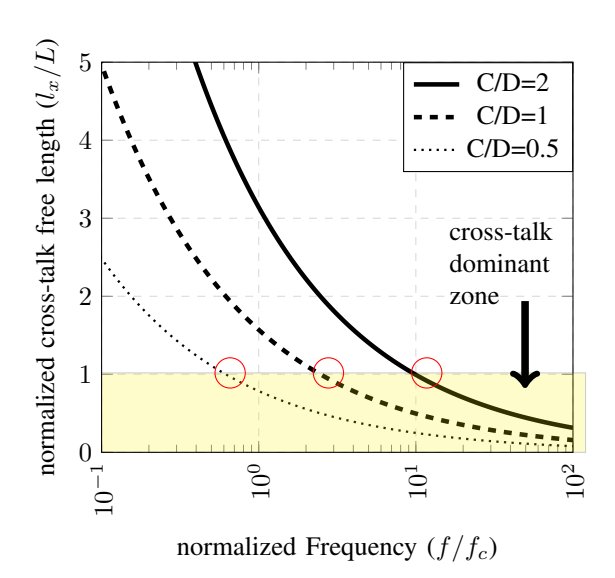


Fig. 2: Normalized interconnect length that can remain free from cross-talk in a group of parallel electrical channels. The frequency scale is normalized with respect to the cut-off frequency of an isolated electrical channel. In y axis, the cross-talk free length is normalized with respect to the physical length of the channel.

is 3 inch, the ratio of wire-width to inter-wire spacing is 0.6, relative permittivity of substrate is 3.38, and substrate thickness is 20 mil. The assumption of ideal conductivity of the metal results in noise-free infinite bandwidth of an isolated channel. We will shortly see that, even under such perfect condition, the ability of signal transfer of an interconnect becomes limited by the cross-talk. Figure 4 shows the degree of cross-talk in a 2-channel electrical data-bus. It reveals that, while signal integrity can remain unperturbed at the low frequency regime ( $\leq$  10 GHz), it begins to aggravate at high frequencies, as other undesired signals, especially the far-end cross-talk begins to compete with, or even can exceed the power level of the transmitted signal. Thus, even in the absence of any material loss, and even with the assumption

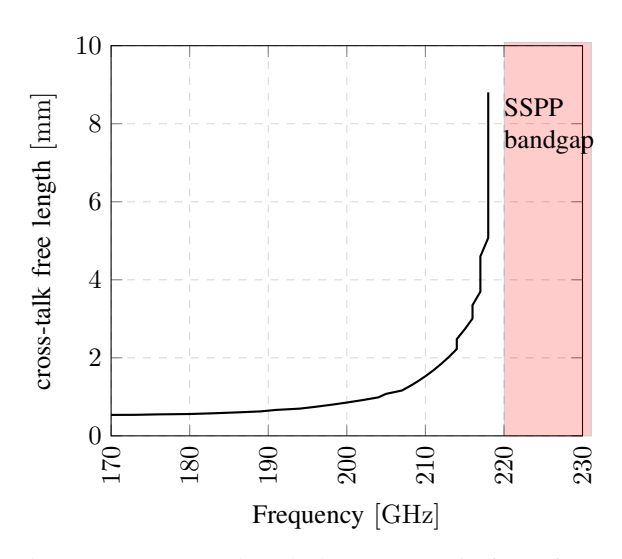


Fig. 3: Interconnect length that can remain free of cross-talk in a group of parallel SSPP channels.

of infinite bandwidth of a standalone channel, the high frequency regime becomes the most troublesome spectrum for data transfer with signal integrity. The loss of signal integrity purely originates from the geometric arrangement of the channels in a densely packed parallel data-bus. In the following section, we shall experimentally demonstrate how the cross-talk-infested high-frequency regime can be recuperated for signal transmission by introducing SSPP parallel data-bus.

## III. EXPERIMENTAL CHARACTERIZATIONS OF SSPP DATA-BUS: ITS RECONFIGURABILITY

SSPP interconnect can accommodate two different kinds of modes: electro-SSPP mode and opto-SSPP mode. In electrical mode, an SSPP channel transfers signal with the assistance of a ground wire. In opto-SSPP mode, a standalone SSPP wire suffices to transport information. Provision of a ground wire is redundant in this mode of operation, as the

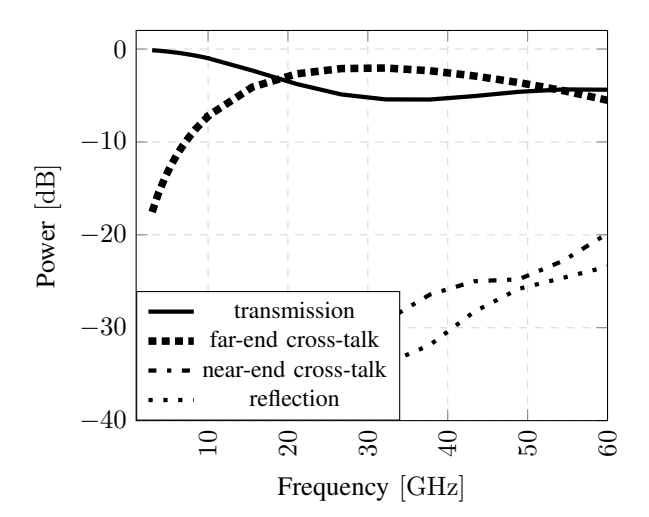


Fig. 4: Near-end and far-end cross-talk in parallel electrical data-bus. At frequencies over 10 GHz, the signal intended to be received at the destination-end of the channel can become indistinguishable from the signal emanating from the cross-talk.

signal sticks to the surface of the metallic wire due to the coupling with the resonant unit cells of metasurface.

In this work, we have experimentally verified both of these mode in a system incorporating parallel data-bus of SSPP waveguide.

#### A. Verification of Electronic-SSPP mode

In order to get a proof-of-concept demonstration of the information capacity of spoof plasmon interconnect we designed a basic SSPP channel with a momentum converter. In actual implementation, the carrier frequency of the channel is envisioned to be hundreds of Gigahertz for ultrafast data transfer. However, for the convenience of measurement, we designed the channel to have a cut-off frequency of 10 GHz. The momentum converter, despite redundant for carrying electrical signal through SSPP channel, will become a necessity when we conduct the experiment on the transport capacity of opto-SSPP signal through the same physical structure. The main section of the designed channels comprises of unit-cells of metamaterial with spoof plasmon resonance frequency at 10 GHz. The electromagnetic scattering properties of the fabricated parallel channels are tested with the channels terminated with standard 50  $\Omega$  input and output resistance. The result of the measurement are shown in Fig. 5, which illustrates the transmission magnitude of a single channel. The transmission coefficient remains almost unity unless we reach the dispersion band-edge of SSPP meta-structure, (in this specific design, at 8.5 GHz). The sharp dip of transmission (-70 dB attenuation) appears at 10 GHz, which is exactly where spoof plasmon resonance is designed. Hence spoof plasmon resonance is a measure of the maximum frequency that can propagate through the metasurface channel.

To measure the far-end cross-talk, we provided signal to the middle channel, measured signal power from the receiving-end of one of the nearest neighbor of the middle channel. The remaining ports were kept open-circuited.

The cross-talk, for most of the part of the band remains below  $-20~\mathrm{dB}$ , which is quite a promising result for designing dense data-bus system for maximizing the bandwidth density. In the low frequency prototype, the space between each pair of neighboring channel is kept twice the length of the groove. In final design for 300 GHz operating frequency, we plan to aggressively scale down this guard space so as to increase the traffic density in the data-bus.

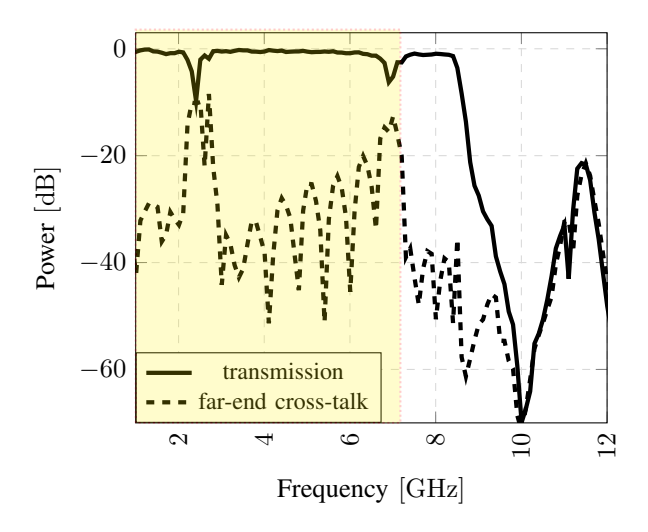


Fig. 5: Experimental verification of the electro-SSPP mode in SSPP channel. The spectral region shown in yellow rectangle corresponds to the electro-SSPP mode. Transmission and cross-talk are measured in a 3-channel parallel data bus

## B. Verification of Optical-SSPP mode

In order to make point to point signal transmission via opto-SSPP mode, we designed an appropriate adapter in the transmitting end so as to convert the transverse electromagnetic mode into a surface bound mode. The adapter comprises of a Vivaldi antenna, and the length of the grooves of the adapter has been gradually increased so as to match the TEM mode with SSPP mode over a broadband. In the receiving side, we employed the mirrored structure of the transmitting adapter. No ground plane is provided at the bottom of substrate, unlike the previous experiment where we tested the transmissibility of electro-SSPP mode.

The dispersion relation of spoof plasmon metasurface suggests that, the field confinement is negligible for frequencies far away from resonance, and the confinement increases as we choose to operate close to resonance. Thus the lower part of the dispersion diagram could not be utilized in a parallel data-bus system for the sake of shielding the neighboring channels from cross-interference. We have shown by an analytical model that the upper 1/3 fraction of the fundamental band of SSPP interconnect can suppress crosstalk during data transfer [5]. For instance, an SSPP data-bus designed from 300 GHz carrier frequency is expected to carry bandwidth of approximately 100 GHz spanning from 200 GHz up to 300 GHz in an optimal set-up.

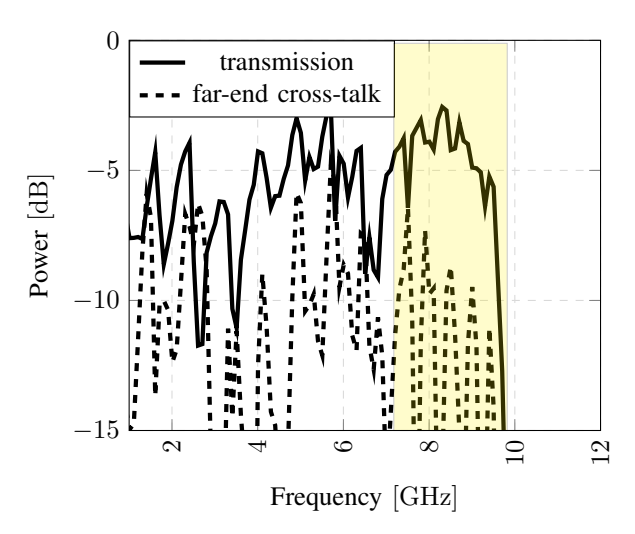


Fig. 6: Experimental verification of the opto-SSPP mode in SSPP channel. Transmission and cross-talk are measured in a 3-channel parallel data bus. The region marked with yellow rectangle indicates the frequency spectrum we can utilize for data transfer with low cross-talk.

In order to verify the nature of cross-talk suppression in our prototype of 10 GHz chip, we provided input signal with 50  $\Omega$  impedance to the centered waveguide of the 3channel system and receive signal from the output terminal of the two remaining side channels. Figure 6 illustrates the measurement result of transmission and far-end cross-talk in an SSPP data-bus. It clearly shows that, as expected from theory, that the low frequency regime is severely plagued by cross-talk to the point that the cross-coupled signal power is almost comparable to the desired transmitted signal level. The cross-talk becomes suppressed as we tend towards the band-edge (in our specific case, band-edge is  $\sim 10$  GHz). A fraction of the transmission spectrum, spanning from almost 7 GHz to 10 GHz in Fig. 6 is shown in yellow rectangular region where the cross-talk remains at least -3 dB low from the signal level. This measurement result substantiates the authors' earlier prediction that, in the circumstances of crosstalk limited bandwidth, an SSPP channel in an optimally designed parallel data-bus can contribute to a maximum of 1/3 band for data transfer while maintaining signal integrity.

Figure 7 shows the microscopic image of the SSPP data bus chip comprising 3 parallel channels with an operating frequency of 300 GHz.

#### IV. RELIABILITY OF SSPP INTERCONNECT

SSPP metasurface derives its unique electromagnetic properties from the careful patterning of the material. From a practical consideration of fabrication process that includes photo-lithography, metallization, rapid thermal annealing and chemical mechanical polishing, the patterns in the fabricated sample may have some variance from the given design. We studied the impact of statistical variation of feature sizes of SSPP channels on its electromagnetic properties. We particularly studied the effect of variance of groove length

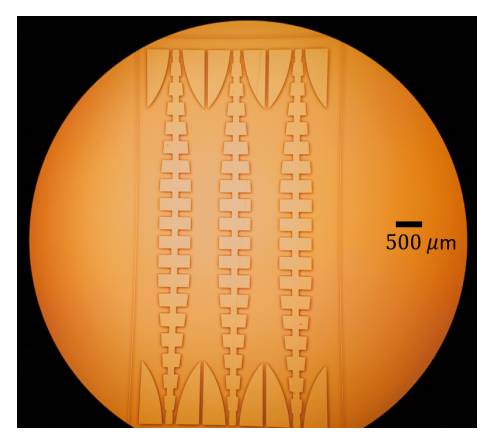


Fig. 7: Optical micrograph of fabricated parallel SSPP channels. The cut-off frequency is designed at 300 GHz.

h, since this is the most critical parameter to determine bandwidth.

In the present study, we designed the groove length (h) such that the resonant frequency  $(\omega_r)$  appears to be close to 300 GHz frequency. The ratio a/d is taken to be 0.3 in order to increase field confinement for a broader range of frequencies on the fundamental band which helps combat cross-talk. We assumed that the process variation would result in a Gaussian distribution of the feature size of SSPP metasurface. In our model, the number of unit cells having groove length h is defined as follows:

$$N(h) = \frac{N_T}{\sigma_h \sqrt{2\pi}} exp\left(-\frac{(h - h_m)^2}{2\sigma_h^2}\right)$$
 (5)

Where  $N_T$  is the total number of unit cells in an SSPP channel,  $h_m$  is the mean value of groove length in the structure, and  $\sigma_h^2 = 1/N_T \sum_i (h_i - h_m)^2$  is the variance of the distribution for h. We have taken the period of the structure to be 375  $\mu$ m, and the groove width is taken as 125  $\mu$ m. The rationale of choosing these value of h parameter follows from the fact that the corresponding resonant frequency of the unit cell is 300 GHz, and this is the spectral ballpark where state-of-the-art sub-terahertz CMOS oscillators can generate carrier frequency efficiently [15], [16]. The value of period d is chosen in a way so that we meet the condition (2h > d)of yielding high field confinement zone of SSPP [7], but at the same time evade the too strong SSPP region where the advantage of strong field confinement is smeared by the drawback of dispersion induced pulse distortion and heightened ohmic loss. The length of each channel is taken as 5 cm.

# V. PERFORMANCE EVALUATION OF FABRICATED NON-IDEAL SSPP INTERCONNECT

Because of random variation of the length of groove in SSPP structure, the transmission characteristics over the frequency range is affected. We defined the bandwidth of a perfect SSPP channel by the difference between the upper  $(f_U)$  and lower cut-off frequency  $(f_L)$ . The upper cut-off frequency is marked by the drop of power gain from the maxima

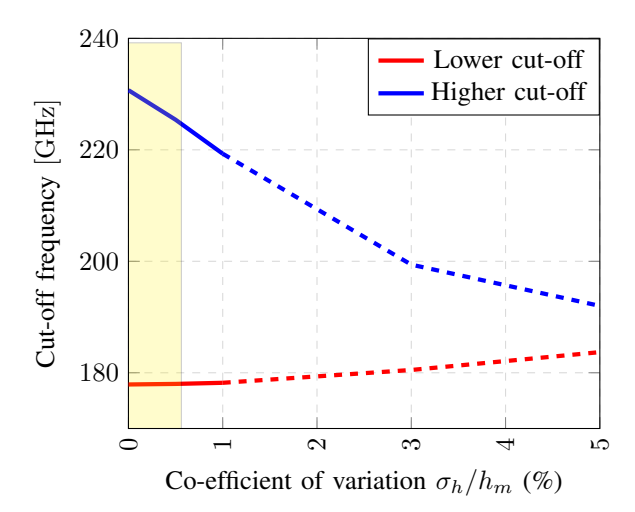


Fig. 8: Change in upper- and lower- cut-off frequencies in crosstalk limited SSPP band. The state-of-the-art fabrication resolution is expected to keep the probable deviation of the bandwidth of fabricated SSPP from the ideal one within the yellow marked region.

by -3 dB, while the lower cut-off frequency is marked by the frequency below which cross-talk power exceeds -3 dB. We observed that the upper cut-off frequency is quite sensitive to the variation of groove length, and shows red-shift with the increase of  $\sigma_h$ . On the contrary, the lower cut-off frequency is relatively less sensitive to the variation of groove length, and shows blue-shift with the increase of  $\sigma_h$ . Figure 8 illustrates the change in upper and lower cut-off frequencies (hence, the corresponding bandwidth reduction) in SSPP transmission spectrum with the increase in coefficient of variation,  $(\frac{\sigma_h}{h_m})$ .

However, the state-of-the-art fabrication process is capable of keeping the coefficient of variance  $(\frac{\sigma}{\mu})$  within a very small range, where  $\sigma$  is the standard deviation and  $\mu$  is the meanvalue of the desired feature size. For instance, in M3 layer of metal in a chip, for a mean value of  $\mu=1$  micron of the metal width, the ratio  $\frac{\sigma}{\mu}$  is reported as 4.6% [17]. For devices with larger feature size, the co-efficient of variation is reasonably expected to be lower. This rationale suggests that, for SSPP interconnect operating at a nominal 1 THz frequency on a silicon substrate, which is characterized by the groove length of roughly 30  $\mu$ m, the ratio of variance to mean value of the feature size will not exceed 0.5 % under state-of-the-art fabrication process.

#### VI. CONCLUSION

With the beginning of the era of tyranny of interconnect, the quest for a novel interconnect technology for inter-chip communication can potentially be satiated by spoof surface plasmon based channel, which can be dynamically adapted between two different modes of information transfer for the sake of maintaining signal integrity at different traffic rate. In this work, we demonstrated both theoretically and experimentally that, SSPP interconnect can be deployed in its electro-

SSPP mode when data-traffic is low, and can be configured to carry opto-SSPP mode when traffic rate becomes high. This action will ensure maximum signal integrity at all traffic rate in a cross-talk limited environment. Not only we cast light on the big promise that spoof plasmon channel makes about its reconfigurability, but also analyze collateral fabrication issues that may emerge with the introduction of the new technology. We believe, this will be marked as an important step towards realization of the novel technology and integrating it with the standard CMOS fabrication process.

#### VII. ACKNOWLEDGMENT

This work was supported in part by the Air Force Office of Scientific Research under Grant No. FA9550-16-1-0363 and in part by the National Science Foundation CISE Research Infrastructure (CRI) under Grant No. F047472.

#### REFERENCES

- M. Zia, C. Zhang, H. S. Yang, L. Zheng, and M. Bakir, Chip-to-chip interconnect integration technologies, IEICE Electron. Express, vol. 13, no. 6, pp. 2016200120162001, 2016.
- [2] K. Saban, Xilinx Stacked Silicon Interconnect Technology Delivers Breakthrough FPGA Capacity, Bandwidth, and Power Efficiency, p. 10, 2012.
- [3] D. A. B. Miller, Are optical transistors the logical next step?, Nature Photonics, vol. 4, no. 1, p. nphoton.2009.240, Jan. 2010.
- [4] Y. Urino et al., First demonstration of high density optical interconnects integrated with lasers, optical modulators, and photodetectors on single silicon substrate, Opt. Express, OE, vol. 19, no. 26, pp. B159B165, Dec. 2011.
- [5] Joy, Soumitra Roy, Mikhail Erementchouk, Hao Yu, and Pinaki Mazumder. "Spoof Plasmon InterconnectsCommunications Beyond RC Limit." IEEE Transactions on Communications 67, no. 1 (2019): 599-610.
- [6] H. Cho, P. Kapur, and K. C. Saraswat, Power Comparison Between High-Speed Electrical and Optical Interconnects for Interchip Communication, J. Lightwave Technol., JLT, vol. 22, no. 9, p. 2021, Sep. 2004.
- [7] M. Erementchouk, S. R. Joy, and P. Mazumder, Electrodynamics of spoof plasmons in periodically corrugated waveguides, Proc. R. Soc. A, vol. 472, no. 2195, p. 20160616, Nov. 2016.
- [8] Joy Soumitra Roy, Yu Hao, and Mazumder Pinaki, Properties of spoof plasmon in thin structures, Proceedings of the Royal Society A: Mathematical, Physical and Engineering Sciences, vol. 474, no. 2220, p. 20180205, Dec. 2018.
- [9] Q. J. Gu, THz interconnect: the last centimeter communication, IEEE Communications Magazine, vol. 53, no. 4, pp. 206215, Apr. 2015.
- [10] J. M. Chamberlain, Where optics meets electronics: recent progress in decreasing the terahertz gap, Philosophical Transactions of the Royal Society of London A: Mathematical, Physical and Engineering Sciences, vol. 362, no. 1815, pp. 199213, Feb. 2004.
- [11] A. Rusina, M. Durach, and M. I. Stockman, Theory of spoof plasmons in real metals, 2010, vol. 7757, pp. 77572R-77572R6.
- [12] G. P. Agrawal, Fiber-Optic Communication Systems, 4 edition. New York: Wiley, 2010.
- [13] D. M. Pozar, Microwave Engineering, 2 edition. New York: Wiley, 1997.
- [14] X. Zhang et al., Heterogeneous 2.5D integration on through silicon interposer, 2015.
- [15] Y. M. Tousi, O. Momeni, and E. Afshari, A 283-to-296GHz VCO with 0.76mW peak output power in 65nm CMOS, in 2012 IEEE International Solid-State Circuits Conference, 2012, pp. 258260.
- [16] R. Han and E. Afshari, A 260GHz broadband source with 1.1mW continuous-wave radiated power and EIRP of 15.7dBm in 65nm CMOS, in 2013 IEEE International Solid-State Circuits Conference Digest of Technical Papers, 2013, pp. 138139.
- [17] K. g. Verma, R. Singh, and B. k. Kaushik, Effects of process variation in VLSI interconnects a technical review, Microelectronics International, vol. 26, no. 3, pp. 4955, Jul. 2009.